Frontiers of Information Technology & Electronic Engineering
www.jzus.zju.edu.cn; engineering.cae.cn; www.springerlink.com
ISSN 2095-9184 (print); ISSN 2095-9230 (online)
E-mail: jzus@zju.edu.cn

Supplementary materials for

Chun GENG, Jiwei LIAN, Dazhi DING, 2023.Compact millimeter-wave air-filled substrate-integrated waveguide crossover employing homogeneous cylindrical lens. *Front Inform Technol Electron Eng*, 24(9):1366-1374. https://doi.org/10.1631/FITEE.2200454

1 Supplement to the operation principle

Suppose that r is the distance away from the center of the homogeneous cylindrical lens (HCL), the theoretical analysis of the proposed crossover can be further deepened using the Green function approach (Gunderson, 1972). Excited by a TE_{10} mode from the air-filled substrate-integrated waveguide (SIW), only the z component of the E-field exists within the parallel waveguide. It can be analyzed that such a case is equivalent to an infinitely long cylindrical lens with a line source. Using a line source excitation at r' and ϕ', the Green function for the lens is the solution to the wave equation in two dimensions. By dividing the area into three zones, the solution is written as

$$\begin{aligned} &G(r,\phi\,|\,r',\phi') \\ &=\sum_n \begin{cases} A_n \mathrm{J}_n(k_1 r)\cos\left[n(\phi-\phi')\right], & r\le a, \\ \left[B_n \mathrm{H}_n(k_0 r)+\varepsilon_n \mathrm{J}_n(k_0 r)\mathrm{H}_n(k_0 r')\right]\cos\left[n(\phi-\phi')\right], & a<r<r', \\ \left[B_n \mathrm{H}_n(k_0 r)+\varepsilon_n \mathrm{J}_n(k_0 r')\mathrm{H}_n(k_0 r)\right]\cos\left[n(\phi-\phi')\right], & r'\le r, \end{cases} \end{aligned} \tag{S1}$$

where J_n represents the Bessel function of the first kind, H_n represents the Hankel function, ϕ represents the rotation angle in the cylindrical coordinate system, n is the order of derivative, ε_n is the dielectric constant, and k_0 and k_1 are the first and second zeros of the Bessel function, respectively. A_n and B_n can be solved by matching the electric and magnetic fields at $r=a$. The E-field can be solved according to

$$\begin{aligned} &E_z(r,\phi|r',\phi') \\ &=\int_c \left[E_z(r_0,\phi')\frac{\partial G(r,\phi|r',\phi')}{\partial n}-G(r,\phi|r',\phi')\frac{\partial E_z(r_0,\phi')}{\partial n}\right]\mathrm{d}\phi', \end{aligned} \tag{S2}$$

where c represents the integral path. By expressing this source field in cylindrical coordinates and integration along $r'=r_0$, the electric field may be written as

$$E_z(r,\phi|r',\phi')=K\sum_n \varepsilon_n(-1)^n\cos(n\phi)\exp\left(\mathrm{j}n\frac{\pi}{2}\right)\left[\frac{\partial P_n(r_0)}{\partial r_0}I_1+P_n(r_0)\left(\mathrm{j}\beta_{10}I_1-\frac{\pi}{\omega}I_2\right)\right], \tag{S3}$$

where

$$K=\left(\frac{2}{\pi k_0 r}\right)^{1/2} D\exp\left[-\mathrm{j}\left(k_0 r-\frac{\pi}{4}\right)\right], \tag{S4}$$

$$P_n(r_0)=C_n \mathrm{H}_n(k_0 r_0)+\mathrm{J}_n(k_0 r_0), \tag{S5}$$

$$C_n = \frac{k_0 \mathrm{J}_n'(k_0 a)\mathrm{J}_n(k_1 a) - k_1 \mathrm{J}_n(k_0 a)\mathrm{J}_n'(k_1 a)}{k_1 \mathrm{H}_n(k_0 a)\mathrm{J}_n'(k_1 a) - k_0 \mathrm{H}_n'(k_0 a)\mathrm{J}_n(k_1 a)}, \tag{S6}$$

$$I_1 = \int_{-\omega/(2r_0)}^{\omega/(2r_0)} \cos\left(\frac{\pi r_0 \alpha}{\omega}\right)\cos(n\alpha)\mathrm{d}\alpha = \frac{2\omega\pi r_0}{(\pi r_0 - n\omega)(\pi r_0 + n\omega)}\cos\left(\frac{n\omega}{2r_0}\right), \tag{S7}$$

$$\begin{aligned} I_2 &= \int_{-\omega/(2r_0)}^{\omega/(2r_0)} \alpha \sin\left(\frac{\pi r_0 \alpha}{\omega}\right)\cos(n\alpha)\mathrm{d}\alpha \\ &= \frac{\omega^2}{(\pi r_0)^2 - (n\omega)^2}\left[\frac{n}{\omega r_0}\sin\left(\frac{n\omega}{2r_0}\right) - 2\frac{(\pi r_0)^2 + (n\omega)^2}{\omega^2}\cos\left(\frac{n\omega}{2r_0}\right)\right]. \end{aligned} \tag{S8}$$

2 Supplement to the design process

Next, parametric study is carried out. Since the designed two-channel crossover is symmetric, we have S_{21}=S_{41}. Here, only S_{11} and S_{21} related to different parameters are investigated. In Figs. S1a–S1h, Figs. S1a–S1d are about S_{11} while Figs. S1e–S1h plot S_{21}. It can be seen that the bandwidth (S_{11}<−15 dB) decreases with an increasing ε_{r2}. As can be seen in Fig. S1b, the thickness h of the substrate has no impact on the reflection loss, as expected. However, the reflection coefficient is highly sensitive to the diameter of the HCL (Fig. S1c), which is selected as a=2.0 mm. The width of the open air-filled SIW influences mainly the feasible bandwidth, as shown in Fig. S1d. For the isolation counterparts, the change in ε_{r2} barely affects the bandwidth of S_{21}, but would shift the frequency range. Similarly, in Fig. S1f, the thickness h of the substrate does not affect the coupling between ports 1 and 2. In Fig. S1g, a maximum bandwidth of S_{21} can be achieved with a=2.5 mm. However, the reflection coefficient deteriorates greatly in this case. Therefore, to balance S_{21} and S_{11}, a=2.0 mm is selected. Considering S_{21} in Fig. S1h, the results would shift related to different w's. Similarly, w=7.2 mm is chosen to balance S_{21} and S_{11}.

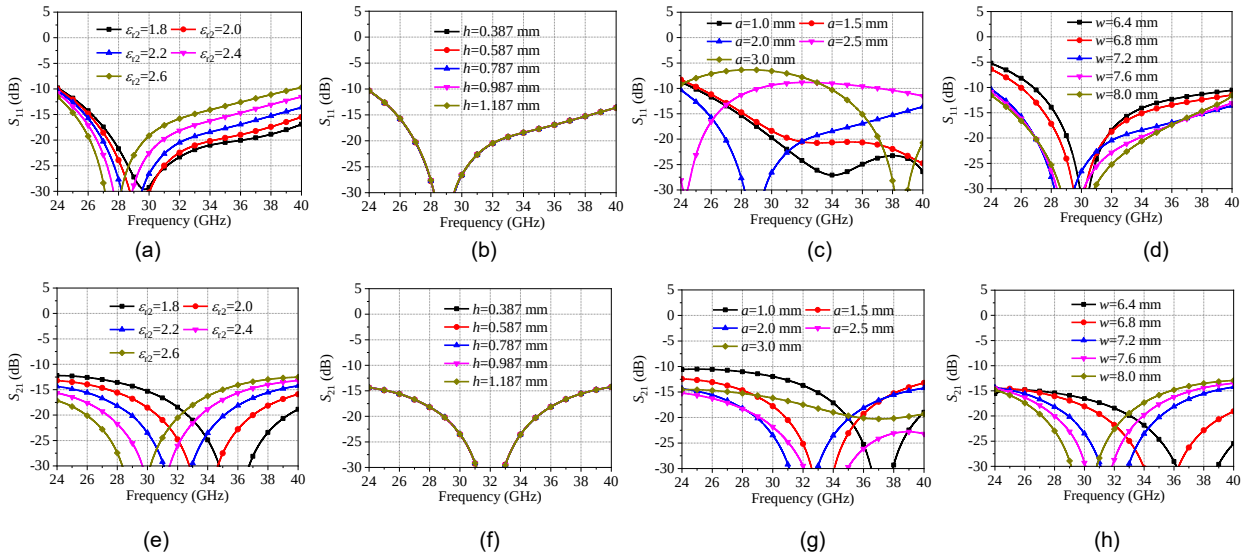

Fig. S1 S_{11} with different ε_{r2} (a), h (b), a (c), and w (d) and S_{21} with different ε_{r2} (e), h (f), a (g), and w (h)

3 Supplement to the experiment

The results of the fabricated three-channel air-filled SIW crossover are plotted in Fig. S2b. A fractional bandwidth (FBW) of 14% is observed in the simulation when the reflection and isolation coefficients are lower

than −15 dB. The measured S_{21} and S_{31} agree well with the simulated counterparts, while the measured S_{11} is deteriorated to about −10 dB. The minimum insertion losses in the simulation and measurement are 1.0 dB and 2.5 dB, respectively.

Similar to the above, the simulated four-channel air-filled SIW crossover has an FBW of 10%, and its reflection and isolation coefficients are below −15 dB from 31.1 to 34.4 GHz. The measured isolation coefficients are in a satisfactory agreement with the simulation results. The bandwidth of the measured S_{11} is reduced to 31.3–33.3 GHz. The simulated and measured maximum insertion losses are 1.1 dB and 3.1 dB, respectively.

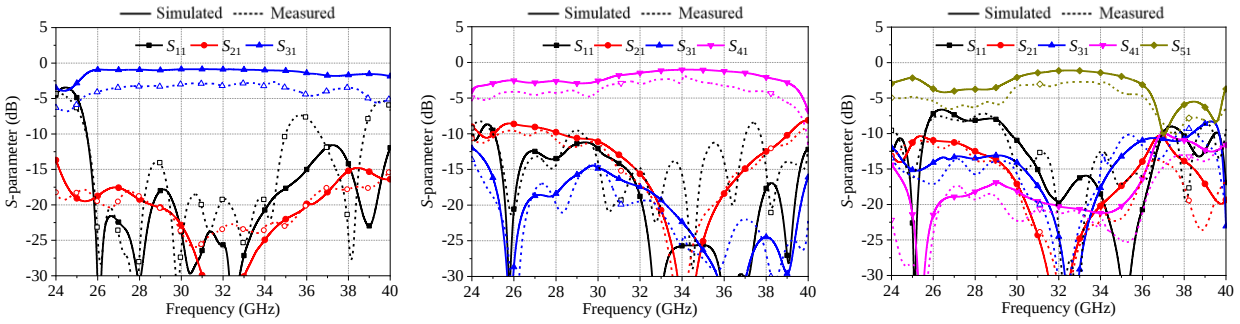

Fig. S2 Simulated and measured *S*-parameters of two-channel (a), three-channel (b), and four-channel (c) SIW crossovers

References

Gunderson L, 1972. An electromagnetic analysis of a cylindrical homogeneous lens. *IEEE Trans Antenn Propag*, 20(4): 476-479. https://doi.org/10.1109/TAP.1972.1140224